

Quantum dots as a probe of fundamental physics: Deviation from exponential decay law

A. Yoshimi, M. Tanaka, and M. Yoshimura
Research Institute for Interdisciplinary Science, Okayama University
Tsushima-naka 3-1-1 Kita-ku Okayama 700-8530 Japan

arXiv:2107.04670v1 [quant-ph] 30 Jun 2021

ABSTRACT

We explore a possibility of measuring deviation from the exponential decay law in pure quantum systems. The power law behavior at late times of decay time profile is predicted in quantum mechanics, and has been experimentally attempted to detect, but with failures except a claim in an open system. It is found that electron tunneling from resonance state confined in man-made atoms, quantum dots, has a good chance of detecting the deviation and testing theoretical predictions. How initial unstable state is prepared influences greatly the time profile of decay law, and this can be used to set the onset time of the power law at earlier times. Comparison with similar process of nuclear alpha decay to discover the deviation is discussed, to explain why there exists a difficulty in this case.

Keywords Exponential decay law and its deviation, Time evolution of resonance electron tunneling, Quantum dot, Semi-classical approximation, Nuclear α -decay, Test of quantum mechanical laws, Exact wave function in parabolic potential

1 Introduction

It is well known that quantum mechanics predicts change of time profile from the exponential to a power law $\propto t^{-p}$, $p > 0$ for times much larger than lifetime defined by the exponential law [1]. The power p may differ in various decay processes [2]. To the best of our knowledge this prediction has never been experimentally confirmed in a definitive way [3], [4]. An exception is a claimed discovery of power law decay in an open quantum system; organic molecules dissolved in solvents which have large relaxation rates caused by interaction of molecules with environment [5]. It is desirable to verify the deviation in pure quantum systems that can neglect interactions with environment. We shall be able to present presumably the best way to verify this prediction by using quantum dots, man-made atoms. A great merit of man-made atoms is that their parameters are better controllable than natural atoms, giving good and easy chances of detecting the deviation at times when remnant atoms are still abundant. We shall compare this method to similar process of nuclear α -decay.

The power law at late times is understood as deviation from the classical Markovian behavior of stochastic process given by the exponential decay in which information at the present time determines all aspects of the future information. The Markovian behavior in the exponential decay is manifest as population ratio at initial time to late times: the ratio of non-decay probability $P(t) = |\langle i|e^{-iHt}|i\rangle|^2$ at a later time t to an earlier time t_0 is a function of time difference; $P(t)/P(t_0) = \exp[-(t - t_0)/\tau]$ with τ the lifetime in the exponential decay period. On the other hand, the power law satisfies an equation, $\ln(P(t_1)/P(t_2)) = -p \ln((t_1 - t_p)/(t_2 - t_p))$ in which $t_p (\gg \tau)$ is an estimated transition time from the exponential to the power law. This formula would reflect that quantum mechanics remembers what happened at time prior to t_p . If one finds a non-Markovian behavior quite different from this formula predicted by the power law, this might suggest a breakdown of quantum mechanical law. In this sense experimental verification of the power law may be regarded as a test of quantum mechanics. At earliest times of decay process the non-decay probability $P(t)$ should behave as an even function of time, $1 - O(t^2)$ due to hermiticity of hamiltonian operator H [6] unlike the one $1 - t/\tau$ that the exponential decay law predicts. From technical difficulty of determining the onset time of decay process experimental study of earliest time behavior is more challenging. We would say somewhat ironically, that the intermediate time behavior of exponential decay law becomes a kind of golden rule, which however must be modified both at earliest and late times.

The main reason we use quantum dots as a tool of exploring fundamental physics is controllability of atomic parameters, basically atomic size and potential depth [7]. Atomic level spacing and their electric dipole moments in natural atoms are tightly correlated by dominant nuclear Coulomb force, but in man-made atoms they are determined by a human choice of optimized dot size and depth (and barrier height) of potential well. We shall consider the size in the range $1 \sim 100$ nm, the potential depth and the barrier height in the range $0.1 \sim 50$ eV. Basic properties of atoms are worked out in one-dimensional quantum well and results may readily be extended to three-dimensional quantum dots. Typical well structures we consider are illustrated in Fig(1) for conceptual one and Fig(2) for more realistic ones. We shall consider quantum tunneling from a resonant state of electron confined within surrounding barrier. The situation is similar to alpha (^4He) particle tunneling in unstable nucleus through the Coulomb barrier, but electron resonance energy and its wave function in man-made atoms are better calculable.

This paper is organized as follows. In Section 2 we lay out description of the space-time evolution of electron tunneling using the semi-classical approximation. The exponential decay law, along with determination of tunneling resonance energy and decay width, is derived by imposing an appropriate boundary condition. In the next Section 3 we examine how the power decay law is derived in a class of semi-realistic potential models and derive transition time t_p from the exponential to the power law. It is possible to predict potential parameter dependence of transition time. In ideal circumstances the transition time may become $O(10)$ times lifetime of the exponential decay law. In Section 5 we examine how preparation of electron resonance influences the time profile of decay law. Both continuous wave and pulse laser irradiation changes the time profile, and we clarify how this can be used to make it easier detection of deviation from the exponential decay. In Appendix A we present exact solution of the Schroedinger problem for parabolic

potential, which helps to clarify subtle points in the semi-classical approximation. Appendix B discusses a problem for potential having cusp structure. Appendix C explains the late time behavior of nuclear alpha decay extending the Gamow potential often used in textbooks.

In a series of works we develop experimental principles of table-top atomic experiments for fundamental physics using quantum dots. In another work [8] we investigate a possibility of measuring parity violation in potential between electrons.

Throughout the present work we use the natural unit of $\hbar = c = 1$ unless otherwise stated.

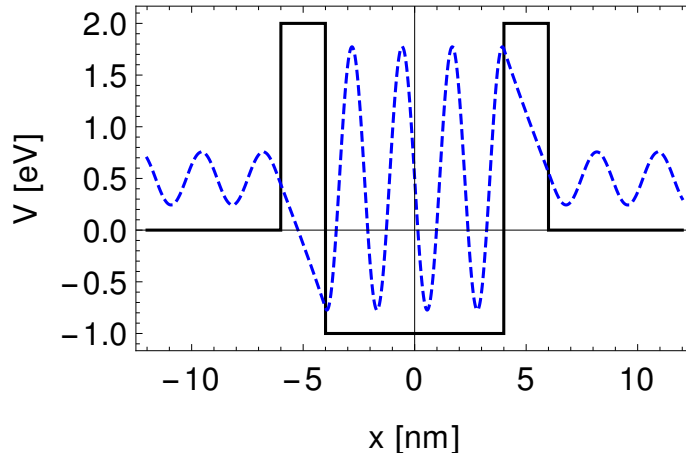


Figure 1: Simplest example of electron tunneling in a potential well surrounded by two barriers to create resonant states whose wave function is illustrated in dashed blue.

2 Space-time evolution of electron tunneling viewed as resonance decay

We consider one dimensional potential well surrounded by two barrier walls: its simplest example is illustrated in Fig(1). It may be more realistic to think of smoothed out potential as in Fig(2). One can consider the problem thus set as an idealization of more complicated two dimensional well in which one dimensional electron motion is frozen in the lowest energy level.

The formula we are based on is the semi-classical time dependent wave function [9] given by

$$\psi(x, t) = \int dE f(E) \frac{\exp[-iEt]}{\sqrt{k(x)}} (c_+(E) \exp[iW(x; E)] + c_-(E) \exp[-iW(x; E)]) , \quad (1)$$

$$W(x; E) = \int_0^x dy k(y) , \quad k(y) = \sqrt{2m(E - V(y))} . \quad (2)$$

We imagine a wave packet of weight factor $f(E)$ centered around a resonance energy $E = E_*$. The formula is appropriate for the wave function inside the well, and $x = 0$ is taken as a center of potential symmetric under $x \leftrightarrow -x$. The asymmetric potential can also be considered, but for simplicity we consider the symmetric case, since the asymmetric case does not give any new insight into physics issues. $c_{\pm}(E)$ terms give right-moving and left-moving waves, respectively, and parity eigenstates dictate $c_{\pm}(E) = \pm c_{\mp}(E)$ for coefficients of parity quantum numbers \pm . From a historical reason the semi-classical approximation is also called the WKB approximation, or the WKB method.

The wave function in the well is usually connected to wave functions under barriers and to those outside barriers, using the linearized potential near the classical turning points given by the equation, $V(x) = E$, since the semi-classical approximation breaks down at turning points. There are four turning points which

are denoted by $\pm a(E), \pm b(E)$ with $b(E) > a(E) > 0$. The linearized potential near these turning points is parametrized as

$$V(x) - E = -V'_a(a - x), \text{ near } x = a, \quad = -V'_b(x - b), \text{ near } x = b, \quad (3)$$

both of $V'_{a,b}$ being positive.

Time independent Schroedinger equation in the linear potential can be exactly solved in terms of well-known Airy functions, denoted by $A_i(x)$ and $B_i(x)$, and connection formulas are often derived by using these exact solutions. We quote connection formulas inside the well and outside two barriers [9]:

$$\psi(x; E) = \frac{A}{\sqrt{k_0(x)}} \exp[i \int_b^x k_0(y) dy] + \frac{B}{\sqrt{k_0(x)}} \exp[-i \int_b^x k_0(y) dy], \quad -a < x < a \quad (4)$$

$$\leftrightarrow \frac{F}{\sqrt{k(x)}} \exp[i \int_a^x k(y) dy] + \frac{G}{\sqrt{k(x)}} \exp[-i \int_a^x k(y) dy], \quad x > b \quad (5)$$

$$\leftrightarrow \frac{J}{\sqrt{k(x)}} \exp[-i \int_{-a}^x dy k(y)] + \frac{H}{\sqrt{k(x)}} \exp[i \int_{-a}^x dy k(y)], \quad x < -b, \quad (6)$$

$$\begin{pmatrix} A \\ B \end{pmatrix} = \frac{1}{2} \begin{pmatrix} 2\theta + \frac{1}{2\theta} & -i(2\theta - \frac{1}{2\theta}) \\ -i(2\theta - \frac{1}{2\theta}) & 2\theta + \frac{1}{2\theta} \end{pmatrix} \begin{pmatrix} F \\ G \end{pmatrix} = \frac{1}{2} \begin{pmatrix} (2\theta + \frac{1}{2\theta}) e^{iL} & -i(2\theta - \frac{1}{2\theta}) e^{iL} \\ -i(2\theta - \frac{1}{2\theta}) e^{-iL} & (2\theta + \frac{1}{2\theta}) e^{-iL} \end{pmatrix} \begin{pmatrix} H \\ J \end{pmatrix}, \quad (7)$$

$$\theta = \exp\left[\int_a^b dy \sqrt{2m(V(y) - E)}\right], \quad L = \int_{-a}^a dy \sqrt{2m(E - V(y))}. \quad (8)$$

As a means of resonance production we consider a pulsed or CW (continuous wave) laser irradiation which can excite a bound electron confined in the well to a resonance state. Resonance state is characterized by no incoming wave boundary condition from outside regions. This boundary condition implies that $G = 0$ and $H = 0$, which gives two conditions,

$$(4\theta^2 + \frac{1}{4\theta^2}) \cos L - 2i \sin L = 0, \quad (9)$$

$$\frac{F}{J} = -i(4\theta^2 - \frac{1}{4\theta^2}) \cos L + 2 \frac{4\theta^2 - \frac{1}{4\theta^2}}{4\theta^2 + \frac{1}{4\theta^2}} \sin L \approx 2 \sin L. \quad (10)$$

The first equation coincides with the equation that determines the complex resonance energy $E_* - i\Gamma_*/2$ where the real part E_* is given by the Bohr-Sommerfeld condition of $L = (n + 1/2)\pi$ (the same semi-classical condition for bound state energies). For a rectangular potential well

$$E_* = \frac{\pi^2}{8ma^2} (n + \frac{1}{2})^2 + V_0, \quad (11)$$

$$\Gamma_* = \frac{1}{4mb^2\theta^2}, \quad \theta = \exp\left[\int_a^b dy \kappa(y)\right], \quad \kappa(y) = \sqrt{2m(V(y) - E_*)} = \sqrt{2m(V_1 - E_*)}. \quad (12)$$

We assumed that the penetration factor θ is very large, hence the decay rate is suppressed by $1/\theta^2$.

Exponential decay law follows in a straightforward manner by considering barrier penetration after resonance excitation. A useful approximation for this purpose is to insert the complex resonance energy, $E = E_* - i\Gamma_*/2$ in the exponent of eq.(1) extended to the region at a far right by the no incoming wave condition $c_-(E) = 0$, to derive (with a normalization of $F = 1/\sqrt{2\pi}$)

$$\psi(x, t; E_*) \sim \frac{f(E_*)c_+(E_*)\Delta E}{\sqrt{2\pi}\sqrt{k_*}\theta} e^{ik_*(x-b) - iE_*t} \exp\left[-\frac{\Gamma_*}{2} \left(t - \frac{x-b}{v_*}\right)\right] \theta\left(t - \frac{x-b}{v_*}\right), \quad (13)$$

$$|\psi(x, t; E_*)|^2 \simeq \frac{|f(E_*)c_+(E_*)|^2 \Delta E^2}{k_*} 4mb^2\Gamma \exp\left[-\Gamma_* \left(t - \frac{x-b}{v_*}\right)\right] \theta\left(t - \frac{x-b}{v_*}\right), \quad (14)$$

where $v_* = \sqrt{2E_*/m}$ is the electron velocity at resonance and the wave packet width is assumed to satisfy $\Delta E \gg \Gamma_*$, but much less than the resonance spacing.

It is however well known that the exponential decay is not the whole story of decay laws [1], [2]. We shall clarify how late time deviation from the exponential decay arises in potential models, using the space-time evolution of resonance electron tunneling.

3 Potential model and decay law at late times

We consider the following type of potentials characterized by three size parameters a, b, Δ and an overall potential value V_w .

$$V(x) = -V_w \frac{1 - (x^2 + a^2)/b^2}{1 + \exp[(x^2 - a^2)/\Delta^2]}, \quad \sqrt{2}a > b > a, \quad V_w > 0. \quad (15)$$

The inequality on sizes, $1 < b/a < \sqrt{2}$, is necessary to provide surrounding barriers. Adopting the middle point value of this inequality, we take $b/a = (\sqrt{2} + 1)/2$. Even with this restriction there are a variety of potential shapes, as illustrated in Fig(2).

Potential shapes: $b = (\sqrt{2} + 1)a/2$

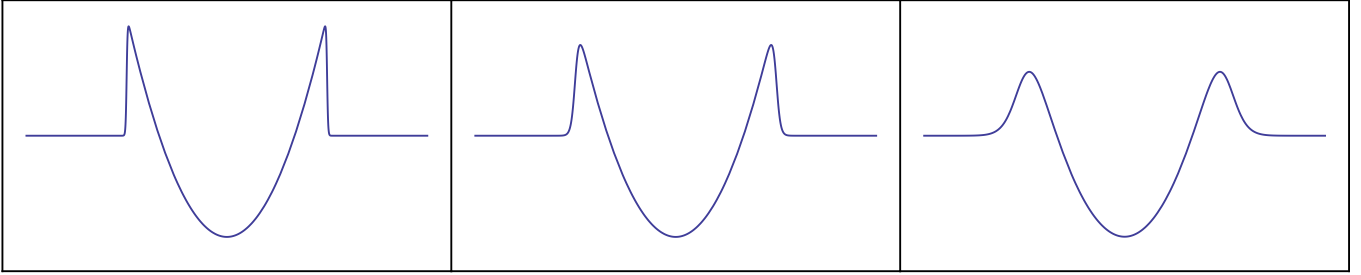


Figure 2: Illustration of potential shapes for $b/a = (\sqrt{2} + 1)/2$: $(a, \Delta) = (5, 0.5)$ nm in the left, $(5, 1)$ nm in the middle, and $(5, 2)$ nm in the right.

This type of potentials consist of three important parts: (1) central well part around $x = 0$, (2) two barrier regions around $x = \pm x_{\max}, x_{\max} > 0$, (3) outside regions of zero potential. The central part is approximately described by harmonic oscillator (HO) potential given by

$$V_c(x) = -V_w(C_0 - C_2 x^2), \quad C_0 = \frac{b^2 - a^2}{b^2(1 + e^{-a^2/\Delta^2})}, \quad C_2 = 2e^{a^2/\Delta^2} \frac{b^2 - a^2 + \Delta^2(1 + e^{a^2/\Delta^2})}{b^2\Delta^2(1 + e^{a^2/\Delta^2})^2}. \quad (16)$$

Energy levels of HO are given by equally spaced eigenvalues,

$$E_n = \omega_0(n + \frac{1}{2}) - C_0 V_w, \quad \omega_0 = \frac{2}{b} \sqrt{\frac{2V_w}{m} \frac{\sqrt{e^{a^2/\Delta^2} (\frac{b^2 - a^2}{\Delta^2} + 1 + e^{a^2/\Delta^2})}}{1 + e^{a^2/\Delta^2}}}. \quad (17)$$

The same formula can also be applied to resonances of energies E_* by using the semi-classical formula of Bohr-Sommerfeld condition,

$$2 \int_{-c}^c dx \sqrt{2m(E_* - V_c(x))} = (n + \frac{1}{2})\pi, \quad (18)$$

with $\pm c$ tuning points given by $V_c(\pm c) = E_*$. For an example given by parameters of Fig(3), we find $E_n = 0.6025\text{eV}(n + 1/2) - 2.5935\text{eV}$, $\omega_0 = 0.6025\text{eV}$, taking $m = 0.1m_e$. A useful parameter n_0 may be introduced by a fractional number at which the bound state energy vanishes:

$$E_n = \omega_0 (n - n_0), \quad n_0 = \frac{C_0 V_w}{\omega_0} - \frac{1}{2}. \quad (19)$$

$n > n_0$ for resonance energy $E_* = E_n$.

Decay widths of resonances are determined by applying the boundary condition of no incoming wave from the outside, to derive the decay width of n-th resonance ($n > n_0$),

$$\Gamma_n = \frac{\omega_0}{\pi} \theta^{-2}, \quad \theta^{-2} = \exp[-4\pi \left(\frac{m}{|V''(x_{\max})|} \right)^{1/2} (V_{\max} - E_n)], \quad (20)$$

$$\Gamma_n \simeq 4.00 \times 10^{15} \text{sec}^{-1} \frac{\text{nm}}{b} \sqrt{\frac{V_w}{10\text{eV}}} \exp[-4.56 \left(\frac{10\text{eVnm}^{-2}}{|V''(x_{\max})|} \right)^{1/2} \frac{V_{\max} - E_n}{\text{eV}}] \frac{\sqrt{e^{a^2/\Delta^2} \left(\frac{b^2 - a^2}{\Delta^2} + 1 + e^{a^2/\Delta^2} \right)}}{1 + e^{a^2/\Delta^2}}. \quad (21)$$

The formula of decay rate, eq.(20), has a simple interpretation: by writing the angular frequency $\omega_0 = 2/T_0$ in terms of classical oscillation period T_0 moving within the well, electron has tunneling probability θ^{-2} each time electron arrives at either of two turning points. In specific examples we consider below the lifetime given by $1/\Gamma_*$ ranges widely, of order psec to nsec, or even wider.

The barrier part near potential tops is well described by parabolic potential, or inverted harmonic oscillator (IVHO):

$$V_b^\pm(x) = V_{\max} - \frac{|V''(x_{\max})|}{2} (x \mp x_{\max})^2. \quad (22)$$

Without loss of generality we take the right part of potential at $x \geq 0$, for which two classical turning points are given by $V_b^\pm(x_\pm) = E$, $x_+ > x_-$ for motion of energy $E = k^2/2m$. Exact solutions of stationary (namely, time independent) Schroedinger equation for parabolic potentials are given by Weber's functions, which are described in Appendix C. In the present section we shall give results of the semi-classical approximation modified by a phase term adopting a feature of exact result.

We apply the semi-classical connection formula of complex coordinate method [10] to wave functions for states near a discrete resonance, applicable for the parabolic potential:

$$\psi_b(x; E) = (m|V''(x_{\max})|)^{-1/8} \frac{e^{-\pi a_u^2}}{(u^2 - a_u^2)^{1/4}} \exp\left[\frac{i}{2} \left(u\sqrt{u^2 - a_u^2} + a_u^2 \ln u^2 \right)\right], \quad (23)$$

$$u = (m|V''(x_{\max})|)^{1/4} (x - x_{\max}), \quad a_u^2 = 2 \left(\frac{m}{|V''(x_{\max})|} \right)^{1/2} (V_{\max} - E). \quad (24)$$

The barrier penetration factor $1/\theta^2$ is related to the exponential here by $\theta^{-2} = e^{-2\pi a_u^2(E)}$. This formula is applicable only in a positive x region of limited $x - x_{\max}$ range. As explained in Appendix A, the phase term proportional to $\ln u^2$ is added by comparing with exact solution of parabolic potential. Remarkably, every detail in the following can be worked out from this formula.

The space-time evolution at late times is described by a time dependent wave function; introducing a wave packet weight $f(E)$, it is

$$\Psi_b(x, t) = \int dE f(E) \psi_b(x; E) e^{-iEt} \equiv \int dE f(E) \exp[i\Phi_b(E; x, t)], \quad (25)$$

$$\Phi_b(E; x, t) = \frac{1}{2} u \sqrt{u^2 - a_u^2} + i\pi a_u^2 + \frac{i}{4} \ln(u^2 - a_u^2) - Et. \quad (26)$$

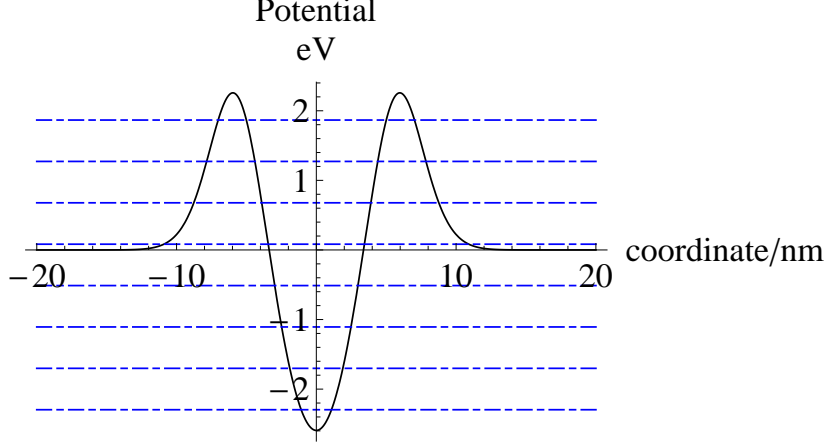


Figure 3: Potential $V(x)$ based on the formula, eq.(15), taking a parameter set: $a = 5\text{nm}$, $b = (\sqrt{2} + 1)a/2$, $\Delta = 4\text{nm}$, $V_w = 10\text{eV}$. Potential maximum is 2.2573 eV, while potential minimum is - 2.5935 eV. All resonances and bound state levels are shown in dash-dotted blue.

Note energy dependence via $a_u^2(E)$. One can estimate this energy integral by the saddle point method. The exponent function $\Phi_b(E; x, t)$ has a saddle point E_s at

$$\left(\frac{\partial \Phi_b(E; x, t)}{\partial E} \right)_{E=E_s} = 0 \Rightarrow$$

$$E_s \simeq V_{\max} - \frac{|V''(x_{\max})|}{2} (x - x_{\max})^2 + \frac{m}{8} \left(\frac{x - x_{\max}}{t} \right)^2. \quad (27)$$

The first two terms in E_s give the parabolic approximation of potential $V_b(x)$ around its top. The last term is numerically small, since $\approx 7 \times 10^{-8} \text{eV} (x - x_{\max})^2 / (\text{nm})^2 (\text{ps}/t)^2$, but its presence is important to late time behavior. When x is close to the turning point and the last term is neglected, the saddle E_s coincides with resonance energy E_* .

The gaussian width around E_s and the amplitude at the saddle are given by

$$\frac{1}{2} \left(\frac{\partial^2 \Phi_b}{\partial E^2} \right)_{E=E_s} \approx \frac{m}{2|V''(x_{\max})|} u (u^2 - a_u^2(E_s))^{-3/2} = \frac{4}{m} \frac{t^3}{(x - |x_{\max}|)^2}, \quad (28)$$

$$\text{with } u^2 - a_u^2(E_s) \simeq \frac{m}{4} \sqrt{\frac{m}{|V''(x_{\max})|}} \left(\frac{x - x_{\max}}{t} \right)^2, \quad (29)$$

$$i\Phi_b(E_s) = iW_0(E_s) - 2\pi \sqrt{\frac{m}{|V''(x_{\max})|}} (V_{\max} - E_s), \quad W_0(E_s) = \frac{u}{2} \sqrt{u^2 - a_u^2(E_s)} - E_s t. \quad (30)$$

The gaussian integral around the saddle gives amplitude and probability for the power law decay,

$$\Psi_{\text{power}}(x, t) \simeq e^{-i\pi/4} \sqrt{\frac{\pi}{2}} f(E_s) \frac{(x - |x_{\max}|)^{1/2}}{t} \exp[iW_0(E_s) - 2\pi \sqrt{\frac{m}{|V''_3(x_{\max})|}} (V_{\max} - E_s)], \quad (31)$$

$$|\Psi_{\text{power}}(x, t; E_*)|^2 \simeq \frac{\pi}{2} |f(E_s)|^2 \frac{x - x_{\max}}{t^2} \exp[-4\pi \sqrt{\frac{m}{|V''(x_{\max})|}} (V_{\max} - E_s)], \quad (32)$$

$$\exp[-4\pi \sqrt{\frac{m}{|V''(x_{\max})|}} (V_{\max} - E_s)] \simeq \exp[-4\pi \sqrt{\frac{m}{|V''(x_{\max})|}} (V_{\max} - E_*)] = \theta^{-2}. \quad (33)$$

This amplitude at late times should be compared to that of the exponential decay period,

$$\Psi_{\text{exp}}(x, t; E_*) \sim \frac{f(E_*)\Delta E}{\sqrt{2}\sqrt{k_*}} e^{ik_*(x-b)-iE_*t} \sqrt{\frac{\Gamma_*}{\omega_0}} \exp\left[-\frac{\Gamma_*t}{2}\right], \quad (34)$$

with $k_* = \sqrt{2mE_*}$ and $x \ll t$. Compared to the decay probability at late times, the exponential decay period gives a corresponding formula,

$$|\Psi_{\text{exp}}(x, t)|^2 \simeq |f(E_*)|^2 (\Delta E)^2 \frac{\Gamma_*}{2\sqrt{2mE_*}\omega_0} \exp[-\Gamma_*t]. \quad (35)$$

Equating two decay probabilities, $|\Psi_{\text{power}}|^2$ and $|\Psi_{\text{exp}}|^2$, we derive equation for transition time t_p

$$\frac{e^{\Gamma_*t_p}}{(\Gamma_*t_p)^2} = \frac{|f(E_*)|^2}{|f(E_s)|^2} \frac{(\Delta E)^2}{\Gamma_*k_*\omega_0(x-x_{\text{max}})} \exp\left[4\pi\sqrt{\frac{m}{|V''(x_{\text{max}})|}}(V_{\text{max}} - E_*)\right]. \quad (36)$$

Let us incorporate the wave packet factor. We consider pulse laser excitation scheme from filled bound state electron to a resonant state. The pulse laser width is denoted by $\Delta\omega = 2\pi\Delta\nu$, which may or may not be larger than resonance decay rate Γ_* . The wave packet factor is defined by weighted state density prepared by laser excitation, hence it is given by

$$f(E) = \frac{(2\pi\Delta\nu)^2/4}{(E - E_*)^2 + (2\pi\Delta\nu)^2/4 + \Gamma_*^2/4}, \quad \Delta E = 2\pi\Delta\nu = \Delta\omega. \quad (37)$$

This leads to

$$\frac{|f(E_*)|^2}{|f(E_s)|^2} (\Delta E)^2 = (\Delta\omega)^2 \left(1 + \frac{4(E_s - E_*)^2}{(\Delta\omega)^2 + \Gamma_*^2}\right)^2. \quad (38)$$

where $2\pi\Delta\nu$ may be identified as ΔE of wave packet width in calculation of space-time evolution of electron resonance decay. As previously mentioned, one may estimate $E_s - E_*$ by taking relevant times $t \geq O(1/\Gamma_*)$, to derive

$$E_s - E_* \leq \frac{m}{8} \Gamma_*^2 (x - x_{\text{max}})^2 \sim 1.1 \times 10^8 \text{sec}^{-1} \left(\frac{x - x_{\text{max}}}{\text{nm}}\right)^2 \left(\frac{\Gamma_*}{\text{ps}^{-1}}\right)^2. \quad (39)$$

We may thus conclude that the ratio, eq.(38), is very close to $(\Delta\omega)^2$, and certainly is not much larger than this value. In the rest of discussion we shall take the ratio to be $(\Delta\omega)^2$.

Combining eq.(36) and eq.(38), we derive for $\xi = \Gamma_*t_p$,

$$\xi - 2 \ln \xi = 4\pi\sqrt{\frac{m}{|V''(x_{\text{max}})|}}(V_{\text{max}} - E_*) + \ln \frac{(\Delta\omega)^2}{\Gamma_*k_*\omega_0(x - x_{\text{max}})} \quad (40)$$

$$\simeq X - 26.86 + \ln \left(\frac{b}{x - x_{\text{max}}} \frac{\Delta\nu}{\text{GHz}} \sqrt{\frac{10\text{eV eV}}{V_w E_*}} \right) \equiv Y, \quad (41)$$

$$X = 8\pi\sqrt{\frac{m}{|V''(x_{\text{max}})|}}(V_{\text{max}} - E_*) \simeq 28.84\sqrt{\frac{\text{eVnm}^{-2}}{|V''(x_{\text{max}})|}} \frac{V_{\text{max}} - E_*}{\text{eV}}, \quad (42)$$

where $k_* = \sqrt{2mE_*}$. Note the important relation, the resonance decay rate $\propto e^{-X/2}$.

The transition region from the exponential to the power law periods may be better described by adding amplitudes in respective regions, to give decay probability,

$$|\Psi_{\text{exp}}(x, t) + \Psi_{\text{power}}(x, t)|^2 \simeq \frac{(f(E_*)\pi\Delta\nu)^2\Gamma_*}{2k_*\omega_0} |e^{-\Gamma_*t/2 - iE_*t} + e^{-i\pi/4} e^{-iE_*t} \frac{e^{-Y/2}}{\Gamma_*t}|^2, \quad (43)$$

with $e^{-Y/2} = 0.02105$ in our example potential. Around the transition time $t = t_p$, there exists an oscillation intrinsic to interference given by the angular frequency of $E_* - E_s$, estimated by

$$E_* - E_s \approx \frac{m}{8(\Gamma_* t)^2} (\Gamma_* (x_+ - x_{\max}))^2 \simeq 1.1 \text{ sec}^{-1} \left(\frac{x_+ - x_{\max}}{\text{nm}} \right)^2 \left(\frac{10 \text{ nsec}}{t} \right)^2, \quad (44)$$

valid for times $t > O(1/\Gamma_*)$. In numerical estimates given below one may take this phase difference nearly vanishing: $E_s \approx E_*$.

We have examined several cases of parameter choices to numerically compute, taking $\Delta\omega/2\pi = 1$ GHz, to derive resonance lifetime, ξ and $e^{-\xi}$ (remnant fraction). For this purpose we fix, for simplicity, $b = (1 + \sqrt{2})a/2$ taking the half-distance of allowed edges of required inequalities, $1 < b/a < \sqrt{2}$. Effective electron mass is taken to be $0.1m_e$. Numerical procedure for the estimate is to first assume a, Δ in nm unit for dot sizes and potential value V_w , and to numerically compute various quantities such as $n_0, |V''(x_{\max})|, X, \xi, e^{-\xi}$. We would prefer a range of outcomes from our own judge of experimental easiness; $1/\Gamma_* = \text{msec} \sim \text{nsec}$ for lifetimes and $e^{-\xi} > 10^{-10}$ for remnant fraction. An example that clears these conditions is illustrated below.

$(a/\text{nm}, \Delta/\text{nm}, V_w/\text{eV})$	$E_*/\text{eV} (n, n_0)$	$1/\Gamma_*$	$ V''(x_{\max}) /\text{eV nm}^{-2}$	X(RHS)	ξ	$e^{-\xi}$	ω_γ/eV
(5, 4, 10)	1.272 (6, 3.86)	17 ns	0.83	15.59 (7.72)	12.8	2.7×10^{-6}	1.784

The last column shows laser photon energy from a bound electron of $n = 3$ to a resonance state $n = 6$. The potential given by this parameter set is depicted in Fig(3) along with all discrete levels. Decay time profile is shown in Fig(4).

Exponential \rightarrow Power law

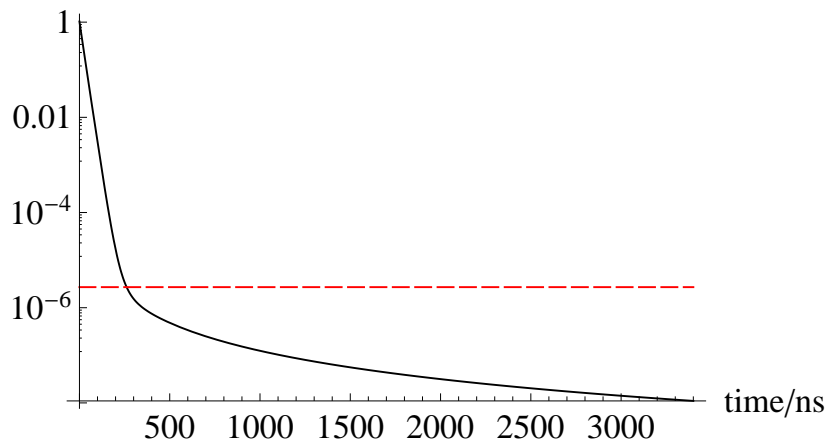


Figure 4: Time profile of decay law according to absolute value part of eq.(43). The horizontal line is population at the transition time.

Our quantum system predicts the late time power to be two, while results in an open system [5] give a variety of late time powers. It is difficult to provide definite theoretical model for this open system.

In Appendix B we discuss decay law in partially linear potential similar to the Gamow potential of nuclear α decay and present a problem of late time behavior. Appendix C presents improved potential

model for nuclear α decay. There is a difficulty of estimating the wave packet weight ratio in this case. Moreover, the remaining right hand side factors already give difficulty of measuring deviation from the exponential decay in nuclear α decay. Much freedom and controllability of electron tunneling in quantum dots give more promising opportunities for the new discovery.

4 Improved results based on exact numerical solutions of one dimensional Schroedinger equation

There are computer softwares to numerically solve the eigenvalue problem of one-dimensional Schroedinger equation for a given potential. Our results using the same set of dot parameters in the previous section are as follows. We listed for comparison results of harmonic approximation, too.

n	E/eV	Γ/eV	HO $E(\Gamma)/\text{eV}$
0	-2.28	0	-2.296
1	-1.67	0	-1.7015
2	-1.06	0	-1.107
3	-0.472	0	-0.512
4	0.0909	6.5×10^{-12}	0.0827
5	0.640	5.9×10^{-8}	0.677
6	1.16	1.3×10^{-5}	1.272(1.93×10^{-8})
7	1.64	9.6×10^{-4}	1.867
8	2.06	2.5×10^{-2}	2.4615
9	2.43	N/A	None

Resonance energy and their width determination is non-trivial. We solved the Schroedinger equation for one-way boundary condition at right and computed reflection and transmission probability at far left. Energy dependence of this probability shows resonance behaviors at special energies, as shown in Fig(5). From these we determined resonance energy and their width which give results as in the above table. We note as a minor comment that transition probability determined this way corresponds to double barrier penetration, while electron resonance decay after laser excitation is given by a single barrier penetration. Hence a factor 1/2 of resonance decay is required for correct interpretation.

The transition time to the power law period is estimated by using exact results as follows. One calculates X and Y factor using the resonance energy E_* , to derive $X = 34.74$ and $Y = 9.60$, from which one has the transition time and the remnant fraction,

$$t_p = \frac{\xi}{\Gamma_*} = 15.02 \times 5.05 \times 10^{-11} \text{sec} = 0.76 \text{ ns}, \quad e^{-\xi} = 3.0 \times 10^{-7}. \quad (45)$$

Discrepancy between exact results and those of harmonic approximation increases as quantum number increases, because the approximation is based on truncation of potential to power series at the bottom. The discrepancy is copious in particular for resonances. In experimental design one needs radiative transition rate for $|6\rangle \rightarrow |3\rangle$. Using numerically derived wave functions of resonance and bound state as shown in Fig(6), we computed dipole transition amplitude, to obtain

$$|\langle n=3|x|n=6\rangle| = 0.0124 \text{nm}. \quad (46)$$

In the harmonic approximation this matrix element vanishes due to the selection rule $\Delta n = \pm 1$. The semi-classical approximation, on the other hand, gives a rather large value 1.15 nm. We shall use dipole moment given by the numerical computation above. The dipole transition amplitude and energy difference between these states, 1.632eV (to be compared with HO result 1.784eV), give radiative transition rate, $2.55 \times 10^5 \text{sec}^{-1}$.

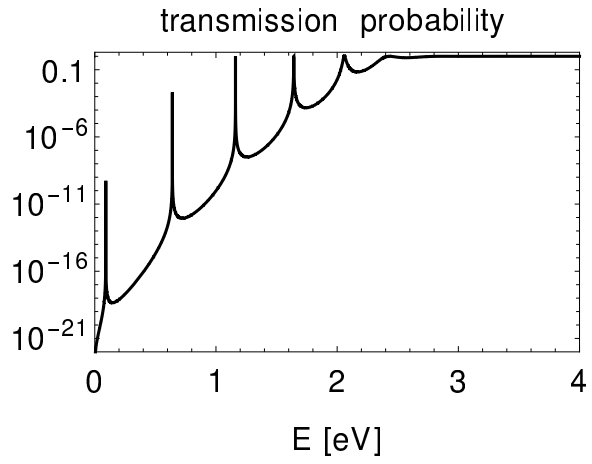


Figure 5: Transmission probability passing double barriers.

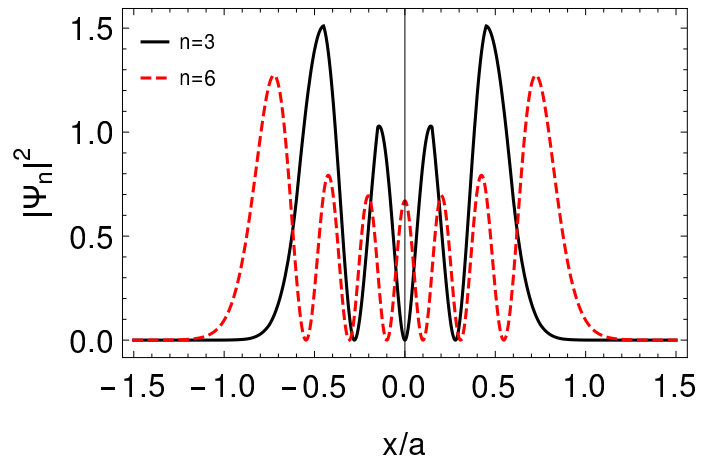


Figure 6: Absolute value of squared wave functions of $n = 6$ resonance in dashed red and $n = 3$ bound state in solid black.

5 Decay law under continuous preparation of unstable states

It was pointed out [15], [16] that rapid and persistent fluctuations such continuous wave (CW) excitation to resonance states may lead to modified late time power decay. The problem is related to that measurements in quantum mechanical systems do depend on how initial states are prepared. We shall study this problem using optical Bloch equation under laser irradiation in electron resonance state that incorporates effectively the power law period as a non-constant decay rate.

We introduce three-level optical Bloch equation for pure system in order to discuss the decay law when resonance state is prepared by laser irradiation. We denote three states by $|i\rangle$, $i = 1, 2, 3$ in which $|1\rangle$ is resonance state, $|2\rangle$ is bound state, and $|3\rangle$ is outgoing plane-wave state in continuum. In the interaction picture we may write two-level OBE under irradiation,

$$\frac{d\sigma_{11}}{dt} = i\frac{\Omega(t)}{2}(\sigma_{12} - \sigma_{21}) - \Gamma_p(t)\sigma_{11} - \gamma_{12}\sigma_{11}(1 - \sigma_{22}), \quad (47)$$

$$\frac{d\sigma_{22}}{dt} = -i\frac{\Omega(t)}{2}(\sigma_{12} - \sigma_{21}) + \gamma_{12}\sigma_{11}(1 - \sigma_{22}), \quad (48)$$

$$\frac{d\sigma_{21}}{dt} = -i\delta_L\sigma_{21} - i\frac{\Omega(t)}{2}(\sigma_{11} - \sigma_{22}) - \frac{\gamma_{12}}{2}\sigma_{21}(1 - \sigma_{22}), \quad (49)$$

$$\frac{d\sigma_{12}}{dt} = i\delta_L\sigma_{12} + i\frac{\Omega(t)}{2}(\sigma_{11} - \sigma_{22}) - \frac{\gamma_{12}}{2}\sigma_{12}(1 - \sigma_{22}), \quad (50)$$

$$\frac{d\sigma_{33}}{dt} = \Gamma_p(t)\sigma_{11}, \quad (51)$$

where γ_{12} is single-photon decay rate $|1\rangle \rightarrow |2\rangle + \gamma$, and

$$\delta_L = \omega_L - \omega_{12}, \quad \Omega(t) = -\langle 2|\vec{d}|1\rangle \cdot \vec{E}(t). \quad (52)$$

Rotating wave approximation is made. The factor $(1 - \sigma_{22})$ is not usually present, but we introduced this term as effect of Pauli blocking of already occupied state. We introduce amplitude time dependence $E_0(t)$ in equation $\vec{E}(t) = E_0(t)e^{i\omega_L t + i\Phi(t)}$ of laser field, but not phase time dependence ($\Phi(t)$ set to zero) for simplicity.

We may choose the power decay formula and laser intensity as follows:

$$\Gamma_p(t) = -\frac{d}{dt} \ln |e^{-\Gamma_* t/2} + e^{-i\pi/4} \pi \frac{\sqrt{k_*(x - x_{\max})}}{2E_*(t + \tau)}|^2, \quad \tau = \frac{1}{\Gamma_*}, \quad (53)$$

$$\Omega(t) = \frac{\Omega_0(t)}{2} \left(1 - \frac{2}{\pi} \text{Arctan} \frac{t - T_1}{\Delta} \right), \quad \Omega_0(t) = \langle 2|\vec{d}|1\rangle \cdot E_0(t). \quad (54)$$

Laser switch-off time T_1 may be taken in a wide range, for instance much less than τ to of order power law transition time. The width Δ is assumed to be of order the laser width $\approx 1\text{GHz}$. The factor τ in the power law amplitude $\propto 1/(t + \tau)$ cannot be precisely fixed, but it should be sufficient for this estimate. It is important to note that radiative E1 decay of $|1\rangle \rightarrow |2\rangle$ is described excellently by the exponential law without the power period.

Since two time scales γ_{12} and transition time $O(10)/\Gamma_*$ are vastly different, one may separate optical Bloch equation into time spans of the laser irradiation and the late time behavior. The first part may be solved by setting $\Gamma_p(t) = 0$ and taking a constant CW laser of time independent Rabi frequency Ω . The steady state solution of $t \rightarrow \infty$ may be derived by taking vanishing derivative, to give

$$\sigma_{11} = \frac{\Omega^2}{4(\delta_L^2 + \gamma_{12}^2/4)}, \quad \sigma_{22} = 1 - \sigma_{11}, \quad (55)$$

$$\sigma_{12} = -\frac{\Omega}{2(\delta_L - i\gamma_{12}/2)} \sigma_{11}. \quad (56)$$

By adjusting Rabi frequency and detuning one may keep a large population of resonance state along with a large coherence with the bound state.

Two interesting limiting cases are then described as follows. The first case concerns a short time termination of laser irradiation. In this case resonance decays both into bound state and outgoing plane wave state. Our special quantum dot case gives a fast radiative decay into bound state, and this reduces greatly the possibility of observing the power decay law of resonance tunneling.

The second case concerns CW laser irradiation over the whole range of power law period. As illustrated in Fig(7), decay process is modified under laser irradiation, without much changing the transition time to the power law period, as in the case of Fig(4). Quantity adopted here as the non-decay probability is $1 - \sigma_{33}(t) = \sigma_{11}(t) + \sigma_{22}(t)$, which contains fast Rabi oscillation between bound state (given by population $\sigma_{22}(t)$) and resonance. We thus see that how preparation of resonance states is made under laser irradiation has a profound effect of controlling the electron resonance tunneling.

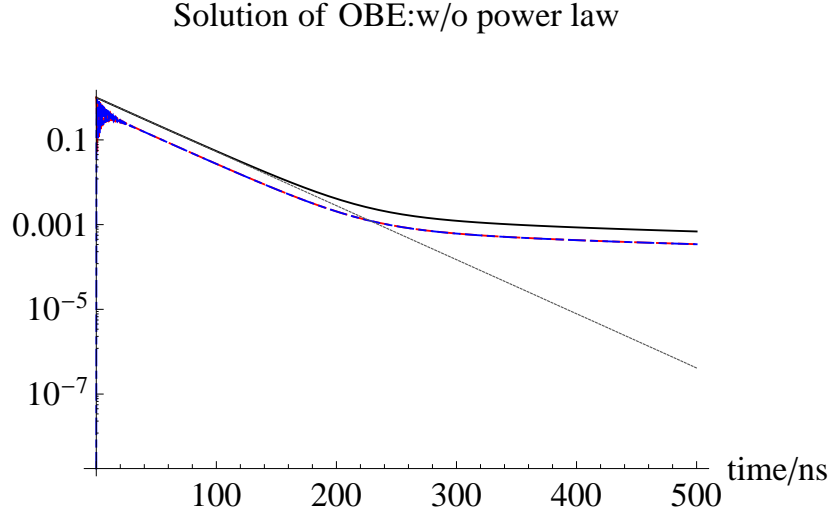


Figure 7: Time profile of non-decay probability given by $1 - \rho_{33}(t)$ (with $\rho_{33} = \sigma_{33}$ total population within quantum dot) under CW laser irradiation of zero detuning: 10 W cm^{-2} in solid black, 1 W cm^{-2} in dashed red, 1 W cm^{-2} without the power law period in dash-dotted blue, and the case without laser irradiation in dotted black.

Duration of pulse laser determines the exponential period as illustrated in Fig(8): shorter pulse expedites onset time of power law period. This way one can control to a certain extent experimental design for discovery of deviation from the exponential decay.

6 Summary

Late time power law has been derived for smooth potentials of electron tunneling in man-made atoms. The late time power law $\propto 1/t^2$ was derived and the transition time t_p is determined in terms of potential parameters, which gives in favorable conditions $O(10) \times$ lifetime of the exponential decay. In man-made atoms, atomic size, potential depth and barrier height can be arranged independently, and this made it possible to derive transition times from the exponential to the power short enough that the power law may be experimentally observed with remnant fractions as large as of order 10^{-7} . The crucial factor for this arrangement is roughly size \times square root of potential height, a typical combination of penetration factor

Solution of OBE:w/o power law

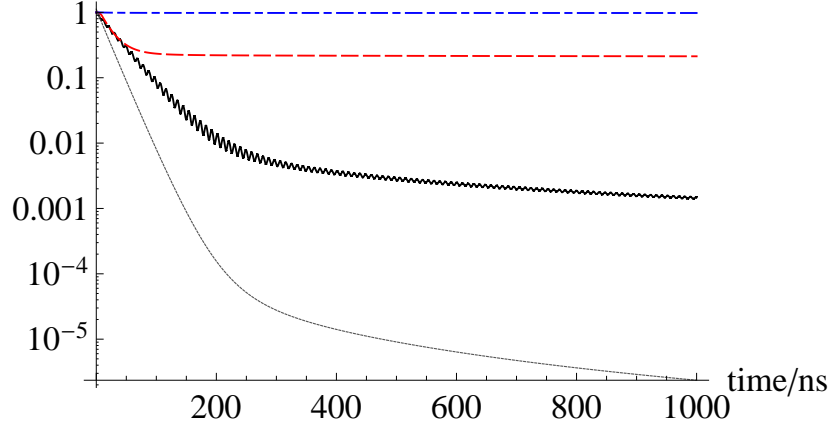


Figure 8: Time profile of decay law $1 - \rho_{33}$ under laser irradiation of zero detuning: 1 W cm^{-2} under CW in solid black, 1 W cm^{-2} under pulse of duration 10 ns in dashed red, pulse 1 W cm^{-2} of duration 1 ns in dash-dotted blue, and the case without laser irradiation in dotted black.

against barriers.

How unstable resonance state is prepared influences the decay law, and we verified this using laser irradiation for transition from bound state. Both CW and pulse laser irradiation changes the time profile of decay law, and duration of pulse influences the onset time of transition to the power law. This helps discovery of deviation from the exponential decay.

A similar tunneling decay, nuclear alpha decay, is predicted to obey the same power law $\propto 1/t^2$, but has experimental difficulty due to a large transition time from the exponential to the power law. We have also examined radiative atomic decay, nuclear beta decay, and some other decay processes, but in all cases it is difficult to find a promising possibility of experimentally observing deviation from the exponential decay law. Man-made atoms give a unique and interesting opportunity of studying deviation of the exponential decay at late times.

7 Appendix A: Exact solutions of the Schroedinger equation for parabolic potential

The stationary Schroedinger equation of energy E in a parabolic potential

$$-\frac{1}{2m} \frac{d^2\psi}{dx^2} + (V(x) - E)\psi = 0, \quad V_2(x) = V_1 - \frac{|V_0''|}{2}x^2, \quad (57)$$

with $V_1 > 0$, may be transformed to Weber's differential equation,

$$\frac{d^2w}{dz^2} + \left(\lambda + \frac{1}{2} - \frac{z^2}{4}\right)w = 0, \quad (58)$$

by a change of coordinate variable and their parameters,

$$z = \alpha x, \quad \alpha = e^{i\pi/4}(m|V_0''|)^{1/4}, \quad \lambda = -\frac{1}{2} - 2i\left(\frac{m}{|V_0''|}\right)^{1/2}(V_1 - E). \quad (59)$$

Classical turning points for electron moving with energy $E < V_1$ are at

$$\pm a, \quad a = \sqrt{\frac{2(V_1 - E)}{|V_0''|}}. \quad (60)$$

Two independent solutions of Weber's differential equations are Weber's functions denoted by $D_\lambda(z)$ and $D_{-\lambda-1}(iz)$ [13]. These functions can be written in terms of linear combinations of confluent hypergeometric functions $F(\alpha, \gamma; z^2/2)$ of parameters, $(\alpha, \gamma) = (-\lambda/2, 1/2), (1/2 - \lambda/2, 3/2)$.

Using general formulas of asymptotic expansion for confluent hypergeometric functions, one confirms that a specific linear combination of two fundamental solutions gives the boundary condition of no incoming wave at the far right. This solution at $x > a$ is given by, disregarding normalization,

$$\psi(x; E) = \frac{\sqrt{2\pi}e^{i\pi/4}}{\Gamma(\frac{1}{2} - ia_u^2)} e^{-\frac{\pi}{2}a_u^2} D_{-\frac{1}{2}-ia_u^2}(e^{i\pi/4}u) - D_{-\frac{1}{2}+ia_u^2}(e^{i3\pi/4}u), \quad (61)$$

and its leading term at $x \gg a$ is

$$\psi_R(x; E) = \frac{-i}{((m|V_0''|)^{1/4}x)^{1/2}} \frac{e^{-\pi a_u^2}}{(u^2 - a_u^2)^{1/4}} \exp\left[\frac{i}{2} \left(u\sqrt{u^2 - a_u^2} + a_u^2 \ln u^2\right)\right], \quad (62)$$

$$a_u = (mV_0'')^{1/4}a = \left(\frac{m}{|V_0''|}\right)^{1/4} \sqrt{2(V_1 - E)}, \quad u = (m|V_0''|)^{1/4}x. \quad (63)$$

The formula $e^{-\mathcal{P}_b}$, $\mathcal{P}_b = \pi(m|V_0''|)^{1/2}a^2$ may be regarded as an effective barrier penetration factor for the parabolic potential. On the other hand, the leading term at $x \ll -a$ is given by

$$\frac{2ie^{i\pi/4}}{((m|V_0''|)^{1/4}|x|)^{1/2}} \cos\left(\frac{1}{2}(u\sqrt{u^2 - a_u^2} + a_u^2 \ln u^2) + \frac{\pi}{4}\right). \quad (64)$$

Using the asymptotic formula of exact solution, one may estimate the probability at turning points, $x = \pm\sqrt{2(V_1 - E)/|V_0''|} \equiv \pm a$, to give

$$\frac{1}{(m|V_0''|)^{1/4}a} \exp[-2\pi(m|V_0''|)^{1/2}a^2] = \sqrt{\frac{\pi}{\mathcal{P}_b}} \exp[-2\mathcal{P}_b]. \quad (65)$$

In Fig(9) we illustrate exact solution given by Weber's function, which shows that the left side sinusoidal wave goes out of a parabolic potential to a right-moving component alone. The penetration factor $\exp[-\pi(m|V_0''|)^{1/2}a^2/2] = 0.21$ is only modestly small in this example.

Although exact solutions are valuable, its mathematical complexity is often demanding for its full understanding. The semi-classical or WKB approximation is intuitively appealing, giving a clear relation to classical behaviors. The wave functions in classically allowed region of $|x| > a$ is described by linear combinations of running waves; at $x > a$

$$\frac{1}{\sqrt{2m(E - V_2(x))}} \exp\left[\pm i \int_a^x dy \sqrt{2m(E - V_2(x))}\right]. \quad (66)$$

We impose the boundary condition of no incoming wave from the far right, which chooses one of these waves. Connection passing turning points to potential region under the parabolic barrier and then to the left of $x < -a$ can be carried out, following the method of complex coordinate [10]. This connection gives wave function in the far left region of the form similar to eq.(64), except the phase term $\propto \ln u^2 \propto \ln x^2$. In Fig(10) we compare thus modified semi-classical result relative to exact result.

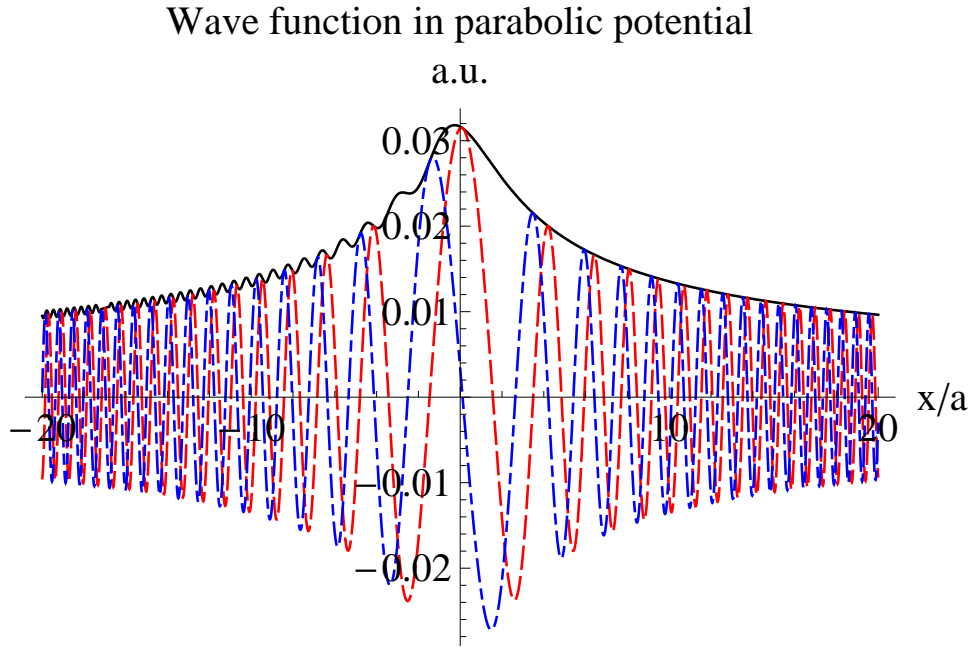


Figure 9: Solution given by Weber's function for $a_u = (m|V_0''|)^{1/4}a = 2$: absolute value in sold black, imaginary part in dashed red, and real part in dash-dotted blue.

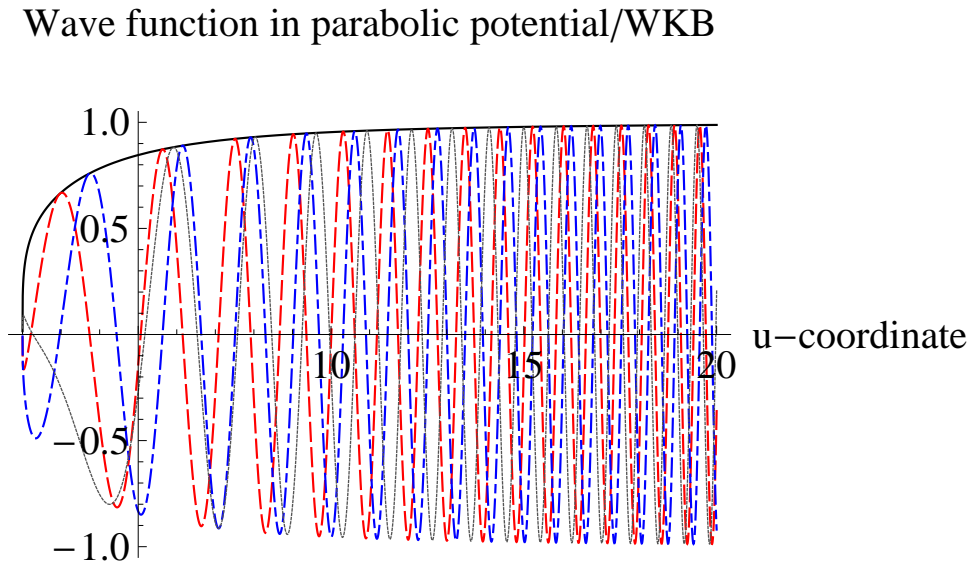


Figure 10: Ratio of exact solution to the semi-classical result in the case of $a_u = (mV_0'')^{1/4}a = 2$: absolute value in solid black, imaginary part in dashed red, real part in dash-dotted blue, and the semi-classical result without $\propto \ln x^2$ phase factor in dotted black.

8 Appendix B: Problem of partially linear potential

We consider a partially linear potential as depicted in Fig(11). It is a $x \leftrightarrow -x$ symmetric potential of the form,

$$V_1(x) = V_1^+(x) + V_1^+(-x), \quad V_1^+(x) = -V_0\theta(a-x)\theta(x) + (V_1 - |V'_a|(x-a))\theta(x-a)\theta(b-x)\theta(x), \quad (67)$$

with V_0, V_1 taken positive. This potential has an aspect of cusp structure (at $x = \pm a$) common to Gamow potential often used in discussion of nuclear α decay. The cusp in Gamow model occurs at nuclear radius.

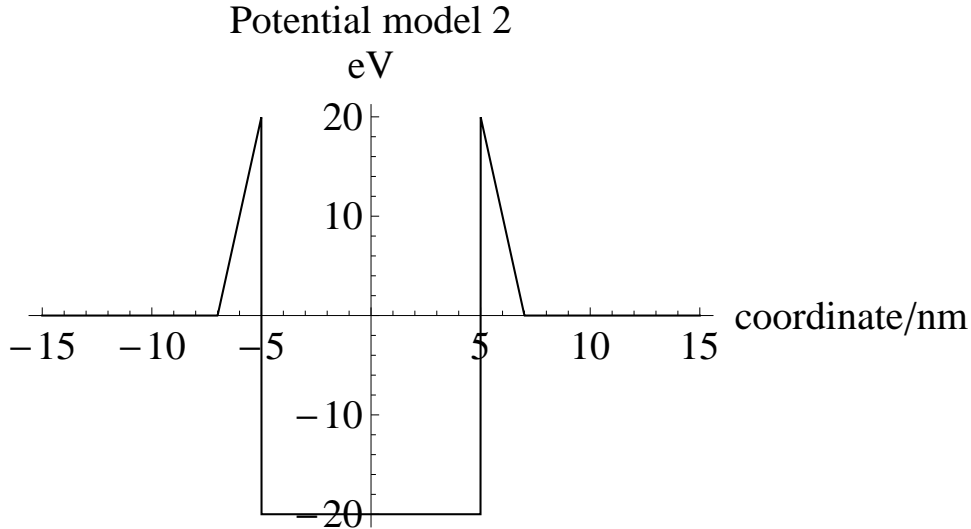


Figure 11: Example of potential given by eq.(67) for the case of $a = 5\text{nm}$, $V_0 = 20$, $V_1 = 20$ eV's, and $V'_a = 20\text{eV}/2\text{nm}$.

Consider the right half $x > 0$ of this potential. Resonance solution is characterized by no incoming wave boundary condition from $x > b$, proportional to e^{ikx} , $k > 0$. Such a solution is given by a linear combination of two Airy functions, $A_i(z)$, $B_i(z)$: at $a < x \leq b$:

$$C_i(x) = N (A_i(\zeta(x)) + iB_i(\zeta(x))), \quad \zeta(x) = \left(\frac{2}{3} \frac{\sqrt{2m}}{|V'_a|}\right)^{2/3} (E - V_1 + |V'_a|(x-a)), \quad (68)$$

with N a normalization constant. This combination of Airy functions has asymptotic behavior given by

$$C_i(x) \propto x^{-1/4} \exp[i\sqrt{2m|V'_a|}x^{3/2}]. \quad (69)$$

As shown in [10], this wave function has a constant flux despite of a fast phase variation $\propto x^{3/2}$.

At a far right of $x > b$ the function $C_i(x)$ is connected to outgoing plane-wave $D(x)$ given by

$$D(x) = C_i(b) \exp[i\sqrt{2mE}(x-b)]. \quad (70)$$

Within the well at $x < a$ the wave function is given by sinusoidal function, either a cosine or sine function depending on parity of states, of variable $\sqrt{2m(E+V_0)}x$. Connection of wave functions at turning points $x = a$ requires matching of logarithmic derivatives:

$$\sqrt{2m(E+V_0)} \left(-\tan(\sqrt{2m(E+V_0)}a), \text{ or } \cot(\sqrt{2m(E+V_0)}a) \right) = \left(\frac{2}{3} \frac{\sqrt{2m}}{|V'_a|}\right)^{2/3} |V'_a| (A'_i(\zeta(a)) + iB'_i(\zeta(a))), \quad (71)$$

two respective equations corresponding to parities of states. This equation determines the resonance energy $E = E_*$.

The asymptotic form of Airy functions is adequately described by semi-classical approximation [10]. The space-time evolution at late times may thus be investigated by working out the semi-classical wave function:

$$\psi(x, t) = \int dE f(E) \frac{c_+(E)}{\sqrt{k(x)}} \exp[i\Psi(E, x)], \quad x > b, \quad (72)$$

$$\Psi(E, x) = W(x; E) - Et, \quad W(x; E) = \int_b^x dy k(y), \quad k(y) = \sqrt{2m(E - V_1(y))}. \quad (73)$$

Estimate of the energy integral in this equation may be given by the saddle point method. Saddles are found by vanishing condition of the phase derivative,

$$\left(\frac{\partial \Psi(E, x)}{\partial E} \right)_{E=E_s} = \pm \frac{\sqrt{2m}}{|V'_a|} (E_s - V_1)^{1/2} + \sqrt{\frac{m}{2E_s}} x - t = 0. \quad (74)$$

Time t is taken large at late times, and the saddle point energy E_s is found of order, $E_s = O(t^2 |V'_a|^2 / m)$. The gaussian width at the saddle necessary for the energy integral is given by

$$\frac{\partial^2 \Psi}{\partial E_s^2} = \pm \frac{1}{2} \frac{\sqrt{2m}}{|V'_a|} (E_s - V_1)^{-1/2} - \frac{1}{4} \frac{\sqrt{2m}}{E_s^{1/2}} x. \quad (75)$$

This gaussian width $|\frac{\partial^2 \Psi}{\partial E_s^2}|^{-1/2}$ is in proportion to $E_s^{1/4} \propto t^{1/2}$ for large E_s , which implies, combined with the pre-factor $1/\sqrt{k} = 1/(2mE_s)^{-1/4}$, a constant decay probability $\propto t^0$, implying that the decay process terminates at latest times after the exponential period. We regard this result inappropriate for description of decay processes. The result was confirmed by using exact Airy solutions as well.

The possibility of a constant decay probability after the exponential period has been noted in a solvable model [14]. In this particular model the non-decay at latest times is attributed to existence of bound state which appears in a strong coupling regime beyond perturbation theory. Our case of partially linear potential model does not correspond to this case of emergent bound state. It is thus not clear under what conditions the behavior of constant decay probability at late times emerges.

9 Appendix C: Late time behavior of nuclear α decay

We clarify late-time profile of α decay by calculating probability amplitude based on Woods-Saxon attractive α -nucleus potential more realistic than the Gamow potential often used in textbooks of nuclear physics. A modified potential is also necessary from result of Appendix B that led to termination of decay process.

9.1 α -nucleus interaction based on Woods-Saxon potential

Consider interaction of α particle (${}^4\text{He}$ nucleus) with residual nucleus, consisting of attractive force inside nucleus and electro static force outside nucleus. We assume that proton or charge distribution inside the residual nucleus has the same form as an attractive Woods-Saxon potential $V_{WS}(r)$,

$$V_{WS}(r) = -V_0 v(r), \quad v(r) = \frac{1}{1 + \exp[(r - R)/a]} = \frac{1}{2} (1 - \tanh \frac{r - R}{2a}) \quad (76)$$

$$V_0 = (51 - 33 \frac{N - Z}{A}) \text{ MeV}, \quad a = 0.67 \text{ fm}, \quad R = 1.27 A^{1/3} \text{ fm}. \quad (77)$$

This potential incorporates a thin nuclear effect instead of cusp at nuclear radius R in the Gamow potential A, Z, N are atomic number, atomic nuclear charge and neutron number of nucleus.

Electro static potential V_C between α and residual nucleus can be calculated from the Poisson equation,

$$\vec{\nabla}^2 V_C = 2(Z-2)e^2 N v(r), \quad N^{-1} = \int d^3 r v(r) = \frac{R^3}{c}, \quad (78)$$

$$\frac{1}{c} = 2\pi \int_0^\infty dx x^2 \left(1 - \tanh \frac{R}{2a}(x-1) \right) = \frac{1}{0.2216} \text{ for } A = 212, \quad (79)$$

$$V_C(r) = \frac{2(Z-2)e^2}{4\pi} N \int d^3 \rho \frac{v(r)}{|\vec{r}-\vec{\rho}|} = \frac{(Z-2)e^2 c}{R^3} \left(\frac{1}{r} \int_0^r dy y^2 + \int_r^\infty dy y \right) \frac{1}{1 + e^{(y-R)/a}}. \quad (80)$$

The constant N is determined by the total charge of α -residual nucleus. The remaining radial integral is expressed in terms of polylogarithmic functions of n-th order, $Li_n(z)$:

$$V_C(r) = -\frac{(Z-2)e^2 c r^2}{Li_3(-e^{R/a}) a^3} J(r), \quad (81)$$

$$\left(\frac{r}{a}\right)^2 J(r) = \frac{\pi^2}{6} + \frac{1}{2}\left(\frac{R}{a}\right)^2 - \frac{1}{6}\left(\frac{r}{a}\right)^2 - Li_2(-e^{(r-R)/a}) + 2\frac{r}{a}Li_3(-e^{(r-R)/a}) - 2\frac{r}{a}Li_3(-e^{-R/a}). \quad (82)$$

The total potential acting on α is given by

$$V_\alpha(r) = V_{WS}(r) + V_C(r). \quad (83)$$

Example of ${}_{84}^{212}\text{Po}$ is illustrated in Fig(12).

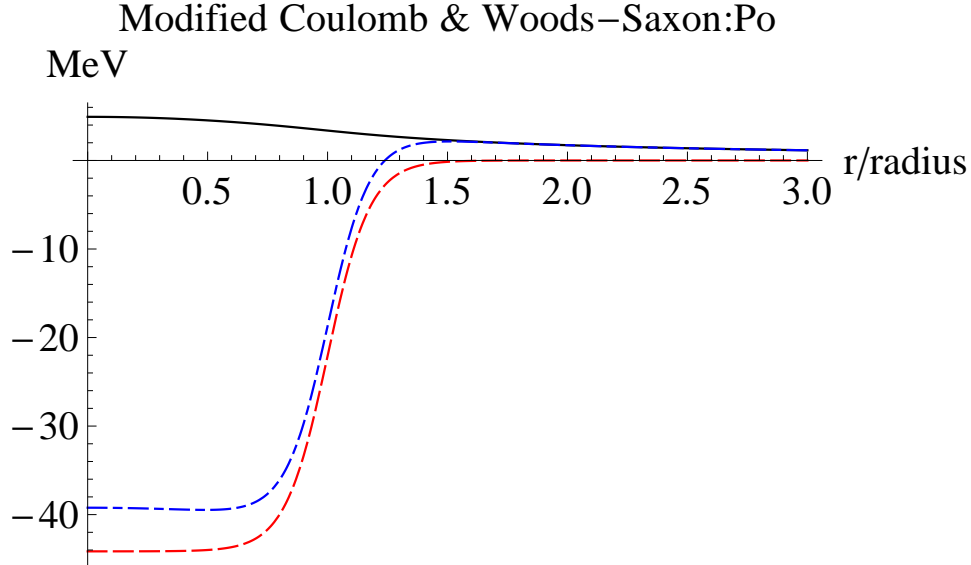


Figure 12: α decay potential of ${}_{84}^{212}\text{Po}$ and its components: modified Coulomb in sold black, Woods-Saxon attraction in dashed red, and their sum in dash-dotted blue.

9.2 Exponential decay law

The time profile of α -decay viewed far away from nucleus is derived using transition amplitude $\mathcal{T}(E)$, a function of α energy E ,

$$\psi_\alpha(r, t) = \int_{-\infty}^{\infty} dE f(E) \mathcal{T}(E) e^{ik(E)(r-R) - iEt}, \quad (84)$$

and is dominated by barrier penetration of α particle. Mechanism of resonant α particle formation is not well understood, but the time evolution is essentially dictated by the boundary condition of no incoming wave from the outside of Coulomb repulsion. This time interval is described in a similar way to resonance formation of electronic state in man-made atoms, and one can assume the formula of eq.(14) adapted to this potential case,

$$\psi_\alpha(x, t; E_*) \sim \frac{f(E_*)C_+(E_*)\Delta E}{\sqrt{2\pi}\sqrt{k_*}\theta} e^{ik_*(x-b)-iE_*t} \exp\left[-\frac{\Gamma}{2} \left(t - \frac{x-b}{v_*}\right)\right], \quad (85)$$

$$|\psi_\alpha(x, t; E_*)|^2 \simeq \frac{|f(E_*)C_+(E_*)|^2\Delta E^2}{k_*\theta^2} \exp\left[-\Gamma \left(t - \frac{x-b}{v_*}\right)\right], \quad (86)$$

$$\theta^{-2} = 4MR^2\Gamma = \exp\left[-2 \int_{-R}^R d\rho \sqrt{2M(V_\alpha - E)}\right], \quad (87)$$

with $C_+(E)$ being the amplitude hitting at the barrier. Details of the potential is irrelevant to the exponential decay law, and the most important factor of barrier penetration factor $1/\theta$ is given in terms of imaginary momentum $\kappa(\rho) = \sqrt{2M(V_\alpha(\rho) - E)}$ integral.

9.3 Late time behavior in the semi-classical approximation and estimate of transition time

Global features of α decay potential are similar to potential form given in Section 4, except energy (MeV vs eV) and size (fm vs nm) scales. The decay probability formula given for electron resonance decay, eq.(32), may be adopted in α decay by appropriate changes of physical quantities from atoms to nuclei.

Estimate of transition time T using $\xi = \Gamma T$ is thus given by

$$\xi - 2 \ln \xi = \ln \frac{\pi r}{2v(V_m)MR^2} + 2 \ln \frac{f(Q)}{f(V_m)}, \quad (88)$$

$$\frac{f(Q)}{f(V_m)} \simeq 1 + \frac{4(V_m - Q)^2}{(\Delta E)^2}. \quad (89)$$

We imagine observations of α particle at a fixed distance r from nuclear targets, taken 1 m in the calculation. The largest target number at transition time is estimated as $e^{-42.98} = 2.16 \times 10^{-19}$ in this example.

A few important features of eq.(88) are

(1) independence of both Q and Γ , which suggests that lifetime of order 1 sec to 1 hour may be of experimental interest.

(2) choice of measurement distance r : distance closer to target region is favored. Additional dependence away from 10 m is $\ln(r/10\text{m})$. At $r = 10\text{cm}$, $\Gamma T = 40.56$, $e^{-\Gamma T} \sim 2.4 \times 10^{-18}$.

(3) atomic mass number dependence $-(2/3) \ln A$, which favors large mass number

Experimental efforts of searching for deviation from the exponential decay have been most extensively focused on nuclear beta and alpha decays. Record search time is $45T_{1/2}$ in nuclear beta decay [4]. and $40T_{1/2}$ in nuclear alpha decay [3] without any positive result for the deviation. There are reasons why the search has met difficulties in these cases.

Acknowledgements

This research was partially supported by Grant-in-Aid 18K03621(MT), 20H00161(AY), and 17H02895 (MY) from the Ministry of Education, Culture, Sports, Science, and Technology.

References

- [1] E. Hellund, Phys. Rev.**89**, 919 (1953).
L.A. Khalfin, Sov. Phys. JETP**6**, 1053 (1958).
For a review, A. Peres, Ann. Phys. (New York) **129**, 33 (1980).
- [2] Various examples of decay law in quantum mechanics and quantum field theory have been given in I. Joichi, Sh. Matsumoto, and M. Yoshimura, Phys.Rev.**58**, 045004 (1998). It is also mentioned that there exists examples lacking the exponential decay period. See also [14].
- [3] Butt and Wilson, J. Phys. **A5**, 1248 (1972).
- [4] E.B. Norman et al., Phys.Rev.Lett. **60** 2246 (1988).
- [5] C. Rothe, S.I. Hintschich, and A.P. Monkman, Phys.Rev.Lett.**96**,163601(2006).
- [6] The argument for this is as follows: $|\langle i|e^{-iHt}|i\rangle|^2 \simeq |\langle i|(1 - iHt - \frac{H^2}{2}t^2 + O(t^3))|i\rangle|^2 \simeq 1 - (\langle i|H^2|i\rangle - \langle i|H|i\rangle^2)t^2 = 1 - t^2 \sum_{n \neq i} |\langle n|H|i\rangle|^2$.
- [7] For a review article on quantum dots, John H. Davies, *The Physics of Low-dimensional Semiconductors* Cambridge University Press (1998).
- [8] M. Tanaka, A. Yoshimi, and M. Yoshimura, *Quantum dots as a probe of fundamental physics: Forbidden radiative transitions due to parity violating interactions*, to appear in arXiv.
- [9] A lucid description of time profile in tunneling decay is given in E. Merzbacher, *Quantum Mechanics*, 3rd edition. Chap.7 "The WKB approximation", Wiley, (1998).
- [10] L.D. Landau and E.M. Lifshitz, *Quantum Mechanics*, 3rd edition, Pergamon Press (1977).
- [11] M.L. Goldberger and K.M. Watson, *Collision Theory* (Wiley, New York, 1964), Chap.8.
- [12] L.A. Khalfin, Sov. Phys. JETP**6**, 1053 (1958).
A. Peres, Ann. Phys. (New York) **129**, 33 (1980).
- [13] E.T. Whittaker and G.N. Watson, *A course of Modern Analysis*, 4th edition, Cambridge (1958).
- [14] D.S. Onley and A. Kumar, Am.J.Phys.**60**, 432 (1992).
- [15] K. Rzazewski, M. Lewenstein, and J.H. Eberly, J.Phys.B: At.Mol.Phys.**15**, L661 (1982).
- [16] P.T. Greenland and A.M. Lane, Phys.Lett.**A117**, 181 (1966)